THE JOURNAL OF BIOLOGICAL CHEMISTRY VOL. 287, NO. 7, pp. 4863–4874, February 10, 2012

G-protein Signaling Modulator-3 Regulates Heterotrimeric G-protein Dynamics through Dual Association with Gβ and $G\alpha_i$ Protein Subunits*[S]

Received for publication, October 7, 2011, and in revised form, December 6, 2011 Published, JBC Papers in Press, December 13, 2011, DOI 10.1074/jbc.M111.311712

Patrick M. Giguère[‡], Geneviève Laroche[‡], Emily A. Oestreich[‡], and David P. Siderovski[‡§¶1]

From the [‡]Department of Pharmacology, [§]Lineberger Comprehensive Cancer Center, and [¶]UNC Neuroscience Center, University of North Carolina School of Medicine, Chapel Hill, North Carolina 27599-7365

Background: GPSM3 is known to bind inactive $G\alpha_i$ and act as a GDP dissociation inhibitor, preventing Gβγ association.
Results: GPSM3 also interacts with Gβ, independent of $G\alpha_i$ binding and excluding a Gγ interaction.
Conclusion: GPSM3 stabilizes Gβ until formation of the Gβγ dimer.
Significance: GPSM3 may establish a novel checkpoint in the regulation of heterotrimeric protein subunit dynamics.

Regulation of the assembly and function of G-protein heterotrimers (Gα·GDP/Gβγ) is a complex process involving the participation of many accessory proteins. One of these regulators, GPSM3, is a member of a family of proteins containing one or more copies of a small regulatory motif known as the GoLoco (or GPR) motif. Although GPSM3 is known to bind $G\alpha_i$·GDP subunits via its GoLoco motifs, here we report that GPSM3 also interacts with the Gβ subunits Gβ1 to Gβ4, independent of Gγ or Gα·GDP subunit interactions. Bimolecular fluorescence complementation studies suggest that the Gβ-GPSM3 complex is formed at, and transits through, the Golgi apparatus and also exists as a soluble complex in the cytoplasm. GPSM3 and Gβ co-localize endogenously in THP-1 cells at the plasma membrane and in a juxtanuclear compartment. We provide evidence that GPSM3 increases Gβ stability until formation of the Gβγ dimer, including association of the Gβ-GPSM3 complex with phosducin-like protein PhLP and T-complex protein 1 subunit eta (CCT7), two known chaperones of neosynthesized Gβ subunits. The Gβ interaction site within GPSM3 was mapped to a leucine-rich region proximal to the N-terminal side of its first GoLoco motif. Both Gβ and $G\alpha_i$·GDP binding events are required for GPSM3 activity in inhibiting phospholipase-Cβ activation. GPSM3 is also shown in THP-1 cells to be important for Akt activation, a known Gβγ-dependent pathway. Discovery of a Gβ/GPSM3 interaction, independent of Gα·GDP and Gγ involvement, adds to the combinatorial complexity of the role of GPSM3 in heterotrimeric G-protein regulation.

G-protein-coupled receptors (GPCRs)[2] are a large superfamily of seven transmembrane domain cell-surface receptors (1–3); the intracellular signals transduced by these heptahelical proteins are themselves tightly controlled by a guanine nucleotide-binding complex of G-protein Gα, Gβ, and Gγ subunits, as well as a growing array of regulatory and accessory proteins (2–6). In the standard model of GPCR signaling, ligand binding to the receptor evokes a conformational change that allows it to convert Gα from the inactive GDP-bound form to the active GTP-bound form (7, 8). GTP-bound Gα dissociates from the Gβγ dimer to further modulate many intracellular effectors such as cAMP-generating adenylyl cyclases and phosphatidylinositol 4,5-bisphosphate-hydrolyzing PLCβ isoforms (9). Signal termination occurs via the intrinsic GTP hydrolysis activity of Gα that restores its GDP-bound state and allows re-association with the Gβγ dimer; a family of "regulators of G-protein signaling" (RGS proteins) can dramatically speed this termination by acting as GTPase-accelerating proteins for various Gα subtypes (4, 6, 10).

In the last few years, multiple discoveries have led to the notion of a more complex regulatory cycle for heterotrimeric G-protein subunits in the cellular context than the standard model mentioned above (5, 6). One of these complexities arose with discovery of the association between inactive GDP-bound $G\alpha_{i/o}$ subunits and GoLoco motif proteins (5, 6, 11), an association that slows the rate of spontaneous GDP release by Gα (12, 13) and excludes formation of the classical Gα·GDP/Gβγ heterotrimer (14, 15). Among the GoLoco proteins originally identified (16–18), one of the smallest at 160 amino acids is GPSM3 ("G-protein signaling modulator type-3"; also known as AGS4 or G18). We and others independently cloned GPSM3 and characterized its guanine nucleotide dissociation inhibitor activity on $G\alpha_i$ subunits (19, 20). This biochemical activity is attributed to the first and third GoLoco motifs (GL1 and GL3)

* This work was supported, in whole or in part, by National Institutes of Health Grants GM082892 from NIGMS (to D. P. S.) and F32 AR057644 from NIAMS (Postdoctoral Fellowship to E. A. O.). This work was also supported by postdoctoral fellowships from the Heart and Stroke Foundation of Canada and Fond de la Recherche en Santé Quebec (to P. M. G. and G. L., respectively).
[S] This article contains supplemental Figs. S1–S3 and "Experimental Procedures."
[1] To whom correspondence should be addressed: Dept. of Pharmacology, School of Medicine, Genetics Medicine Bldg., University of North Carolina at Chapel Hill, 120 Mason Farm Rd., Chapel Hill, NC 27599-7365. E-mail: dsiderov@med.unc.edu.

[2] The abbreviations used are: GPCR, G-protein-coupled receptor; GPSM3, G-protein signaling modulator-3; PhLP, phosducin-like protein; PLC, phospholipase C; BiFC, bimolecular fluorescence complementation; ANOVA, analysis of variance; BRET, bioluminescence resonance energy transfer; CCT, chaperonin containing TCP1; BFA, brefeldin-A; PMA, phorbol 12-myristate 13-acetate; RFP, red fluorescent protein.

of the GPSM3 sequence; we have shown that the second GoLoco motif is inactive because of degeneracy within a critical (E/D)QR triad normally highly conserved within GoLoco motifs (11, 19).

Beyond *in vitro* guanine nucleotide dissociation inhibitor activity and a recent report that GPSM3-Gα_{i1} complex formation can be affected by G-protein-coupled receptor activation (21), very little has been reported about the functional relevance of GPSM3 to cellular signal transduction. Here, we report studies stemming from a yeast two-hybrid screen that identified Gβ subunits as GPSM3 interactors. Expanding its known repertoire of interactors and functions, GPSM3 was found to interact with free Gβ subunits (in a manner not dependent on the established GoLoco motif/Gα_i interaction) and modulate cellular signal transduction via the G$\beta\gamma$ effector PLCβ.

EXPERIMENTAL PROCEDURES

Commercial Antibodies, Constructs, and Other Reagents—Horseradish peroxidase (HRP)-conjugated anti-hemagglutinin (HA) monoclonal antibody (clone 3F10) was obtained from Roche Diagnostics. Anti-β-actin, anti-FLAG M2 antibody, and agarose-conjugated anti-FLAG M2 antibody were purchased from Sigma. HRP-conjugated goat anti-mouse and goat anti-rabbit antibodies were from GE Healthcare. Anti-phospho-Akt (Ser-473) and anti-Akt were from Cell Signaling Technology (Danvers, MA). The expression plasmid for HA-tagged LPA1R was purchased from The Missouri S&T cDNA Resource Center (Rolla, MO). All other cDNAs used in this study were cloned in the pcDNA3.1 backbone vector (Invitrogen) with HA, Myc, or FLAG epitope tag sequences included in the forward PCR primer to produce N-terminally tagged open reading frames. All mutagenesis was performed using the QuikChange site-directed mutagenesis kit following the manufacturer's recommendations (Agilent Technologies, Santa Clara, CA). The two *GPSM3*-specific shRNAs used in this study were developed by The RNAi Consortium and acquired from University of North Carolina Lenti-shRNA Core Facility through Open Biosystems (Huntsville, AL). The pLKO.1 self-inactivating lentiviral vector drives shRNA expression from a human U6 promoter and carries the puromycin-resistance gene under control of a phosphoglycerate kinase promoter. Lentiviruses were produced by transient transfection of pLKO.1 vector plasmids in human HEK293T cells along with packaging plasmid (pCMVΔ8.9) and envelope plasmid (VSV-G pHCMV-G) provided by The RNAi Consortium. Stable THP-1 cell lines expressing *GPSM3*-specific shRNA were produced by lentiviral infection following the protocol of The RNAi Consortium. Briefly, exponentially growing THP-1 cell cultures at low passage were infected with a 1:10 dilution of lentivirus in RPMI 1640 medium (Invitrogen) supplemented with 10% fetal bovine serum (Cellgro, Manassas, VA) and containing 8 μg/ml of Polybrene (Sigma). 48 h following lentiviral infection, puromycin (Sigma) was added at a final concentration of 10 μg/ml, and cells were selected for 8 days.

Anti-GPSM3 Antibody Production—Full-length N-terminally His-tagged human GPSM3 protein was produced recombinantly in bacteria from a pET vector-based prokaryotic expression construct using previously described cloning, expression, and purification techniques (22). Briefly, BL21(DE3) *Escherichia coli* expressing His_6-hGPSM3 was grown to an $A_{600\ nm}$ of 0.8 at 37 °C before induction with 0.5 mM isopropyl β-D-thiogalactopyranoside. After culturing for 14–16 h at 20 °C, cells were pelleted by centrifugation and frozen at −80 °C. Bacterial pellets were then purified using His-Trap FF column chromatography according to the manufacturer's instructions (GE Healthcare) and buffer exchanged into PBS by dialysis. Mouse immunization and hybridoma development to produce the mouse monoclonal anti-GPSM3 antibody 35.5.1 were performed under the auspices of the University of North Carolina Immunology Core (director, Dr. Bradley Bone).

Cell Culture and Transfection—Human embryonic kidney 293 (HEK293), African green monkey kidney fibroblast (COS-7), and THP-1 cell lines were each obtained from the American Type Culture Collection (ATCC) and maintained in DMEM or RPMI 1640 medium (THP-1) (Invitrogen) supplemented with 10% fetal bovine serum (Cellgro, Manassas, VA) at 37 °C in a humidified atmosphere containing 5% CO_2. Transient transfections of cell monolayers grown to 75–90% confluence were performed using Lipofectamine 2000 (Invitrogen) according to the manufacturer's instructions.

Immunoprecipitation and Immunoblotting—Cells were lysed with ice-cold lysis buffer (20 mM HEPES, pH 7.5, 1 mM EDTA, 150 mM NaCl, 1% Nonidet P-40, and Complete protease inhibitor mixture tablets (Roche Applied Science) at 4 °C on a rocker platform for 30 min. Lysates were clarified by centrifugation at 16,000 × *g* for 15 min at 4 °C and quantified by the bicinchoninic acid (BCA) protein content assay (Pierce). For immunoprecipitation, lysates were incubated with specific antibody for 2 h at 4 °C followed by overnight incubation with protein-A/G-agarose (Santa Cruz Biotechnology, Santa Cruz, CA) or directly incubated with agarose-conjugated anti-FLAG M2 antibody overnight. Pelleted antibody-bead complexes were then washed three times with lysis buffer and proteins eluted in Laemmli buffer. Eluted proteins or lysate samples were resolved on 4–12% precast SDS-polyacrylamide gels (Novex/Invitrogen), transferred to nitrocellulose, immunoblotted using primary and HRP-conjugated secondary antibodies, and visualized by chemiluminescence (ECL, GE Healthcare).

Mass Spectrometry Analysis—Immunoprecipitation of FLAG-GPSM3 after cellular co-transfection of FLAG-GPSM3 and HA-Gβ2 DNA constructs was performed as described above from 6 wells of a 6-well plate with agarose-conjugated anti-FLAG M2 antibody overnight and resolved on 4–12% precast SDS-polyacrylamide gels. Gel was fixed and stained with SYPRO Ruby gel stain following the manufacturer's protocol (Invitrogen). The band of interest was excised and sent to MS Bioworks LLC (Ann Arbor, MI) for processing and analysis by nano-LC/MS/MS.

Inositol Phosphate Accumulation Assay—COS-7 and HEK293 cells were seeded in 12-well plates at a density of 1.5×10^5 and 6×10^5 cells per well, respectively. The next day, cells were transfected with DNA plasmids using Lipofectamine 2000 according to the manufacturer's instructions. The following day, cells were metabolically labeled for 18 h with *myo*-[^{3}H]-inositol at 8 μCi/ml in inositol-free DMEM (MP Biomedicals, Solon, OH) containing 0.5% BSA and 20 mM HEPES, pH 7.5. On

the day of the experiment, cells were washed once with phosphate-buffered saline (PBS) and then incubated in prewarmed DMEM (without inositol) containing 0.5% BSA, 20 mM HEPES, pH 7.5, and 35 mM LiCl for 10 min. Thereafter, cells were stimulated with 10 μM lysophosphatidic acid (or vehicle control) for 60 min. Following stimulation, the medium was removed, and the reactions were terminated by addition of 150 μl of 50 mM formic acid and incubation for 1 h at room temperature. Then 50 μl of formic acid supernatant was mixed with 75 μl of 2.67 mg/ml SPA beads diluted in ice-cold water (RNA-binding YSi beads, GE Healthcare) in a 96-well/plate and agitated at 4 °C for 30 min. The radioactivity was counted with a Wallac MicroBeta luminescence counter (PerkinElmer Life Sciences).

Bimolecular Fluorescence Complementation (BiFC)—Fusion constructs were made similar to those previously described for Gβγ tracking (23), namely a fusion of the N-terminal fragment (amino acids 1–158) of yellow fluorescent protein (YN) to the N terminus of full-length GPSM3 ("YN-GPSM3") and the C-terminal fragment (amino acids 159–238) of YFP (YC) to the C terminus of Gβ2 ("Gβ2-YC"). HEK293 cells were transfected with an equal amount of plasmids encoding the fusion proteins YN-GPSM3 and Gβ2-YC, and cells were incubated at 37 °C for 24 h. Total DNA quantity was normalized using empty pcDNA3.1 vector DNA. To measure fluorescence from formed complexes, transfected cells were washed, harvested, and resuspended in PBS. BiFC signal was acquired using a Mithras LB-940 plate reader (Berthold Technologies, Oak Ridge, TN) using an excitation/emission filter set of 485 and 510 nm. The level of expression of each fusion protein was quantified by Western blotting using a polyclonal antibody directed against the GFP.

Bioluminescence Resonance Energy Transfer (BRET)—HEK293 cells were seeded in 12-well plates (3.5×10^5 cells/well) and transfected with a fixed amount of Gβ1-Rluc vector DNA (50 ng) and with increasing amounts of GFP10-GPSM3 vector DNA (0–1500 ng) and corresponding (decreasing) amounts of pcDNA3 empty vector (1500 to 0 ng) to obtain a saturation curve. The competition BRET assay was performed by transfecting cells with 50 ng of Gγ2-RLuc vector, 750 ng of GFP10-Gβ1 vector with 750 ng of FLAG-GPSM3 or pcDNA3 vector, or by transfecting 50 ng of Gβ1-RLuc vector and 750 ng GFP10-GPSM3 vector with 750 ng of HA-Gγ2 or pcDNA3 vector. 24 h post-transfection, cells were washed once, harvested, and resuspended in BRET buffer (phosphate-buffered saline with 1 mM $CaCl_2$, 0.5 mM $MgCl_2$, 0.1% glucose) and distributed in white 96-wells microplates. BRET was initiated by adding coelenterazine 400a at a final concentration of 5 μM. Measurements of emitted light were collected on a Mithras LB-940 plate-reader (Berthold Technologies) using a $BRET^2$ filter set.

Immunofluorescence Confocal Microscopy—HEK293 cells were seeded in a 12-well plate and transfected with 0.4 μg of each DNA, YN-GPSM3 and $Gβ_2$-YC. Then 100 μl of CellLight™ Golgi-RFP Bacman 2.0 (Invitrogen) was added as a Golgi marker. The following day, cells were transferred to a poly-D-lysine-coated coverslip in a 6-well plate and grown overnight. For Golgi disruption, a final concentration of 20 μg/ml brefeldin A (BFA) was added to the cells 15 min prior to fixation. For endogenous protein labeling, 1.0×10^6 THP-1 cells were grown for 72 h on poly-D-lysine-coated coverslips in 6-well plates in the presence or absence of 50 ng/ml phorbol 12-myristate 13-acetate (PMA). Cells were then fixed with 4% paraformaldehyde plus PBS for 10 min at room temperature. Cells were then washed with PBS and permeabilized with 0.1% Triton X-100 plus PBS for 30 min at room temperature. Nonspecific binding was blocked with 0.1% Triton X-100 plus PBS containing 5% nonfat dry milk for 30 min at room temperature. Cells were then incubated with GPSM3-specific mouse monoclonal antibody 35.5.1 (1:100 dilution) and with a pan-Gβ-specific rabbit polyclonal antibody from Santa Cruz Biotechnology (M-14; 1:100 dilution) for 1 h at room temperature in PBS supplemented with 5% nonfat dry milk. Then cells were washed three times with PBS containing 0.1% Triton X-100, followed by incubation with a goat fluorescein isothiocyanate-conjugated anti-mouse secondary antibody and a goat Texas Red-conjugated anti-rabbit antibody (Molecular Probes, Carlsbad, CA) at dilutions of 1:200 for 1 h at room temperature. Cells were then washed three times with permeabilization buffer. Finally, coverslips were mounted using Vectashield mounting medium (Vector Laboratories, Burlingame, CA) and examined by confocal microscopy (Olympus Fluoview FV1000) using a 60× oil immersion objective. Co-localization was assessed by the examination of merged images that showed co-localized regions. In addition to the merged image, an extracted merged pixels picture was generated using Image-Pro software (Media Cybernetics, Bethesda). Images were collected and processed with Image-Pro Plus 6.0 and Adobe Photoshop CS4 software.

RESULTS AND DISCUSSION

Identification of Gβ Subunits as Novel GPSM3 Interacting Partners—In a pilot experiment to test the effects of GPSM3 on cellular GPCR signaling, we found that ectopic GPSM3 expression in HEK293 cells inhibited signaling of the agonist-activated lysophosphatidic acid receptor LPA1R to endogenous PLCβ activation and the generation of inositol phosphate (Fig. 1*A*, *left panel*). Surprisingly, ectopic GPSM3 expression was also found to inhibit PLCβ2 activation by Gβγ dimer stimulation in COS-7 cells (Fig. 1*A*, *right panel*). Currently, the only established binding partners for GPSM3 are Gα subunits of the $G_{i/o}$ family (19, 20, 24).

To help identify additional interacting partner(s) of GPSM3 that might explain its effect on Gβγ-dependent effector activation, we performed a yeast two-hybrid screen. Using full-length GPSM3 as bait, we screened 10^6 human leukocyte cDNA clones from a commercial library. Our screen identified two different clones encoding $Gα_{i2}$, as expected given the two functional Gα$_i$·GDP-interacting GoLoco motifs (GL1 and GL3) present in GPSM3 (amino acids 63–81 and 133–152, respectively (19)). Two different clones of the $Gβ_1$ subunit were also identified in the screen. Fig. 1*B* shows the specific interaction between GPSM3 and $Gβ_1$ in yeast with purified bait and prey clones transfected and yeast grown under auxotrophic selection. Although multiple other GoLoco motif-containing proteins have demonstrated interactions with $G_{i/o}$ family Gα subunits in yeast two-hybrid screens (*e.g.* LGN, Pcp2, and Rap1GAP (25–27)), none of these reports identified Gβ subunits as binding partners.

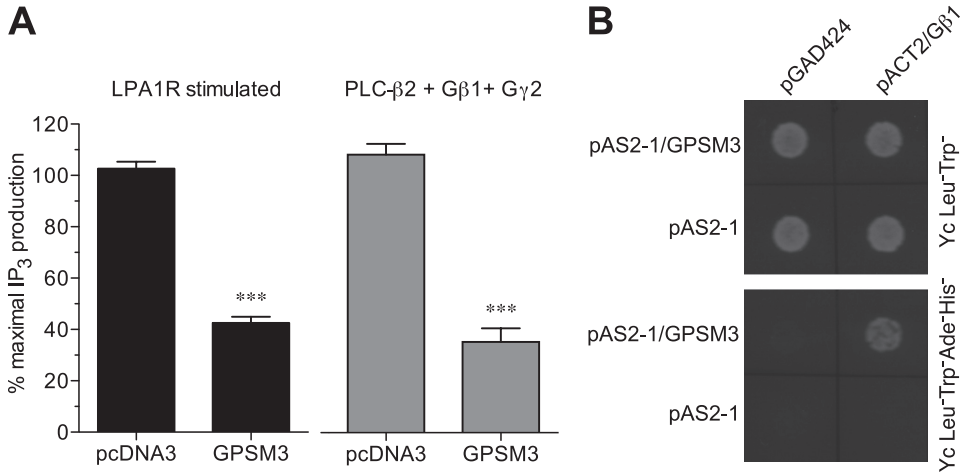

FIGURE 1. **Inhibition of Gβγ-mediated signaling by GPSM3 and identification of Gβ1 as a GPSM3-interacting protein in a yeast interaction trap screen**. *A,* inositol phosphate accumulation was measured in HEK293 cells upon agonist-induced activation of the lysophosphatidic acid receptor LPA1R co-transfected with the LPA1R expression vector and the indicated cDNAs (*left panel*) or in COS-7 cells upon triple co-transfection with expression vectors for PLCβ2, Gβ1, and Gγ2, along with indicated cDNAs. Response was normalized to inositol phosphate accumulation measured in cells transfected with control vector (empty pcDNA3.1). ***, $p < 0.001$ by one-way ANOVA. *B, Saccharomyces cerevisiae* (budding yeast) was co-transformed with indicated bait plasmids (either expressing the Gal4p DNA binding domain alone (*pAS2-1*) or as a fusion with full-length GPSM3 (*pAS2-1/GPSM3*)) and prey plasmids (either expressing the Gal4p activation domain alone (*pGAD424*) or as a fusion with the entire human Gβ1 open-reading frame (*pACT2/Gβ1*)). Transformed yeast were plated onto synthetic defined agar (*Yc*) lacking leucine (Leu^-, to select for the prey plasmid) and tryptophan (Trp^-, to select for the bait plasmid); growth on Yc Leu^- Trp^- medium demonstrates incorporation of both bait and prey plasmids (*top panel*). Growth on Yc Leu^- Trp^- medium also deficient in adenine (Ade^-) and histidine (His^-) indicates a positive protein/protein interaction (*bottom panel*).

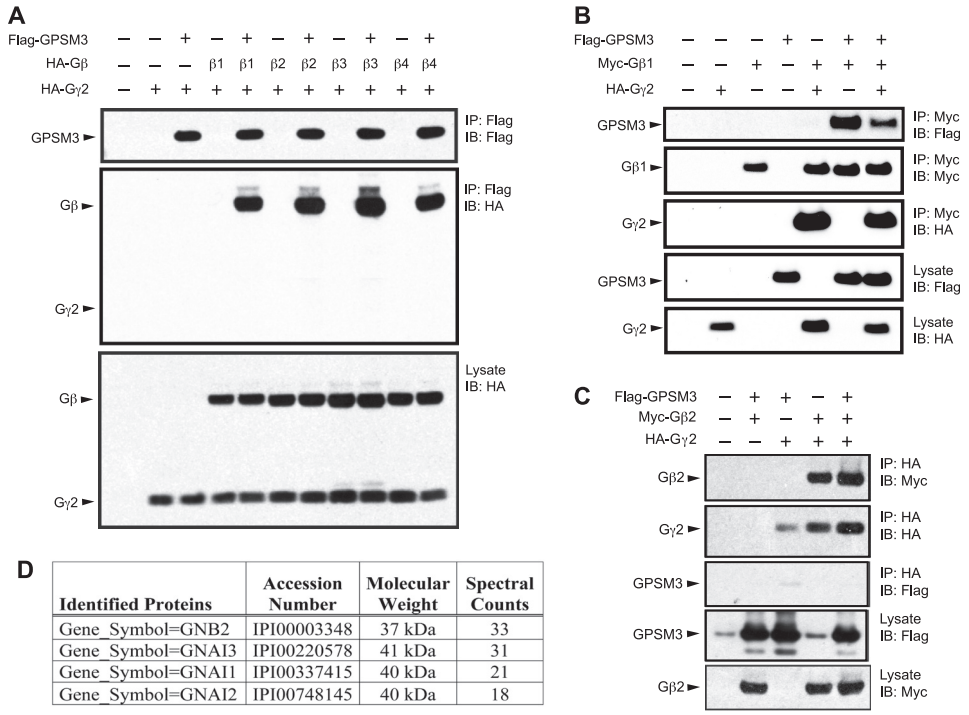

D

Identified Proteins	Accession Number	Molecular Weight	Spectral Counts
Gene_Symbol=GNB2	IPI00003348	37 kDa	33
Gene_Symbol=GNAI3	IPI00220578	41 kDa	31
Gene_Symbol=GNAI1	IPI00337415	40 kDa	21
Gene_Symbol=GNAI2	IPI00748145	40 kDa	18

FIGURE 2. **GPSM3 interacts with all conventional G-protein β subunits and all Gα$_i$ subunits.** *A,* COS-7 cells were transiently co-transfected with plasmids expressing FLAG-tagged GPSM3, HA-tagged Gγ2, and/or HA-tagged Gβ subunits as indicated. Immunoprecipitation (*IP*) of GPSM3 was performed using agarose-conjugated anti-FLAG M2 antibody, and co-immunoprecipitating proteins were detected by immunoblotting (*IB*) with anti-HA epitope tag antibody. All four Gβ subunits (Gβ1 to Gβ4) were observed to co-immunoprecipitate with FLAG-GPSM3, but without concomitant co-immunoprecipitation of the HA-tagged Gγ2 subunit. *B* and *C,* to eliminate a trivial explanation that the absence of detectable HA-tagged Gγ2 was perhaps a technical issue with immunoblotting for such a small polypeptide, the reciprocal co-immunoprecipitation was also performed (*i.e.* immunoprecipitation of tagged Gβ and Gγ subunits). COS-7 cells were co-transfected with Myc-tagged Gβ1 and HA-tagged Gγ2 in the presence or absence of FLAG-tagged GPSM3; resultant cell lysates were immunoprecipitated using a polyclonal anti-Myc (*B*) or monoclonal anti-HA (*C*) antibodies and interacting proteins detected by immunoblotting with anti-Myc, anti-HA-, and anti-FLAG-HRP conjugates. RIPA-buffer solubilized fractions from each co-transfection condition were loaded as controls and marked as *lysate*. All experiments were repeated at least three times with identical results. *D,* HEK293 cells were transiently co-transfected with FLAG-tagged GPSM3 and HA-tagged Gβ2, and immunoprecipitation of FLAG-GPSM3 was performed using agarose-conjugated anti-FLAG M2 antibody. Immunoprecipitates were resolved on a 4–12% NUPAGE SDS-PAGE, and component proteins were visualized by SYPRO Ruby staining, and an apparent band at ~40 kDa was excised for LC/MS/MS peptide sequence identification. The four hits showing the highest spectral counts are shown. Co-expressed Gβ2 shows the highest counts, and all three endogenous Gα$_i$ subunits were also detected.

To confirm this novel discovery of an interaction between GPSM3 and Gβ subunits, we performed co-immunoprecipitation experiments in COS-7 cells. All four conventional Gβ subunits were observed to co-immunoprecipitate with GPSM3 (Fig. 2*A*); given the hematopoietic restricted expression of GPSM3,[3] we excluded analysis of the neuron-specific, Gβ family outlier Gβ5 that is known to associate with R7-RGS proteins rather than conventional Gγ subunits (28). Cell lysates used in these experiments contained no added nucleotide nor aluminum tetrafluoride (*i.e.* performed without forcing any active Gα nucleotide state that could release Gβ protein from intact heterotrimers).

We were surprised to observe that GPSM3 could co-immunoprecipitate with Gβ subunits in the absence of co-immunoprecipitated Gγ subunits; however, there is precedence for this type of interaction, even beyond the Gβ5/R7-RGS protein pairings (28), given that phosducin-like proteins (PhLPs) have been shown to bind monomeric Gβ subunits in their role as chaperones for newly synthesized Gβ proteins prior to their association with Gγ subunits (29, 30). Fig. 2 demonstrates reciprocal co-immunoprecipitation experiments that serve to exclude any technical issue of detecting the small molecular weight Gγ subunit. Immunoprecipitation of Myc-tagged Gβ1 was seen to co-immunoprecipitate either GPSM3 or the Gγ2 subunit (Fig. 2*B*); co-expression of Gβ with both GPSM3 and Gγ slightly diminished the detection of both Gβ-GPSM3 and Gβγ complexes (Fig. 2*B*, *last lane*), whereas immunoprecipitation of HA-tagged Gγ2 co-immunoprecipitates only Gβ without being affected by the presence of GPSM3 (Fig. 2*C*). We also tested other HA-tagged isoforms of Gγ subunits and found that neither $G\gamma_1$, $G\gamma_{11}$, nor $G\gamma_{13}$ was present in immunoprecipitated Gβ-GPSM3 complexes (supplemental Fig. S1).

Tandem mass spectrometry was also used as an independent means to detect GPSM3 complex formation with G-protein subunits. Ectopically expressed FLAG-tagged GPSM3 was immunoprecipitated from HEK293 total cell lysate; the resultant immunocomplex was separated by one-dimensional SDS-PAGE and visualized by subsequent SYPRO Ruby protein gel staining. A predominant band at ~40 kDa was observed, excised, and analyzed by MS/MS. Fig. 2*D* lists the first four hits observed with the highest spectral counts. The Gβ2 subunit was the most prominent protein present in the complex, followed by all three isoforms of $G\alpha_i$ subunits.

Confirmation of the Gβ/GPSM3 Interaction in Cells Using BiFC and BRET—As an additional independent measure of the Gβ/GPSM3 interaction, and to locate this interaction in the cellular context, we used BiFC (31, 32) with split YFP-tagged GPSM3 and Gβ2 fusion constructs. If an interaction occurs between fusion partners (in this case, GPSM3 and Gβ2), the fluorophore of YFP is reconstituted, although the interaction is irreversible, preventing normal interaction dynamics between the two proteins (31, 32). This irreversibility can be advantageous in these studies when two proteins are thought to interact transiently, a property we expect for the Gβ/GPSM3 interaction, given the following: (i) GPSM3 interacts with free Gβ rather than the Gβγ dimer (Fig. 2); (ii) Gγ apparently competes with GPSM3 for Gβ (Fig. 2*B*); and (iii) once formed, the Gβγ dimer is considered indissociable (33, 34), reducing the likelihood that GPSM3 induces Gβγ dimer dissociation.

Expression of each construct alone (YN-GPSM3 or Gβ2-YC) gave minimal observable fluorescence (Fig. 3*A*); expression of each construct with a control counterpart (*i.e.* the paired fluorescent protein fragment without the fusion bait) also gave little fluorescence even at high levels of overexpression (data not shown). When combined, the pairing of YN-GPSM3 and Gβ2-YC expression plasmids yielded a strong cellular fluorescence signal that was inhibited by co-expression of nontagged Gβ2 (Fig. 3*A*), an additional measure of the specificity of the YN-GPSM3/Gβ2-YC interaction.

Subcellular localization of the complex formed between YN-GPSM3 and Gβ2-YC was investigated using confocal microscopy. Two different expression patterns were reproducibly observed when multiple cells were analyzed. One pattern is shown in Fig. 3*B*, *panels a–d*, in which most of the fluorescence from the Gβ-GPSM3 complex is located in the cytoplasm with some co-localization with a Golgi marker (Golgi-RFP; Fig. 3*B*, *panel d*). Co-localization of the two proteins at the Golgi suggests that the initial interaction between GPSM3 and Gβ subunits occurs early during Gβ neosynthesis. The second pattern observed is illustrated in Fig. 3*B, panels e–h*, in which the majority of the fluorescence signal forms an intracellular spot in a juxtanuclear region close to the Golgi marker. To confirm that this pattern of Gβ-GPSM3 complex localization is exclusive of the Golgi apparatus, we treated cells with BFA. Treatment with BFA disrupted the Golgi (Fig. 3*B*, *panels i–l*) as expected (35), but it did not disrupt formation of the Gβ-GPSM3 complex at its juxtanuclear location (*e.g.* Fig. 3*B*, *panel i*).

Based on our findings with YN-GPSM3 and Gβ2-YC co-expression (*e.g.* Fig. 3*B*), the Gβ-GPSM3 complex seems to be formed in and traffic through the Golgi apparatus, but it appears to reside in a distinct structure rather than being trapped in the Golgi when irreversibly tethered via YFP fluorophore reconstitution. This observation is highly reminiscent of aggresome formation- juxtanuclear structures that form around the microtubule organizing center with no or partial co-localization with the Golgi (36, 37). The formation of aggresomes by irreversibly tethered Gβ-GPSM3 complexes is consistent with the idea that BiFC disrupts the normal dynamic interaction that occurs between two proteins and can lead to accumulation of this complex in an inclusion body to protect cells from potentially toxic aggregates (36).

To overcome any bias caused by a loss of normal interaction dynamics in BiFC, we also used BRET to directly monitor the interaction between GPSM3 and Gβ in living cells. The specificity of the interaction was confirmed by a BRET saturation experiment. Expression of a constant amount of a Gβ1-RLuc (*Renilla* luciferase) fusion protein with increasing amounts of GFP10-GPSM3 fusion protein showed a saturable interaction (Fig. 3*C*). Confirming results previously obtained by co-immunoprecipitation (Fig. 2*B*), Gγ2 was seen using BRET to inhibit the complex formation between GPSM3 and Gβ; expression of

[3] Suggestions of a hematopoietic lineage restriction of GPSM3 expression are derived from unpublished observations of M. Branham-O'Connor and J. B. Blumer cited in Ref. 21; see also P. M. Giguère, G. Laroche, and D. P. Siderovski, manuscript in preparation.

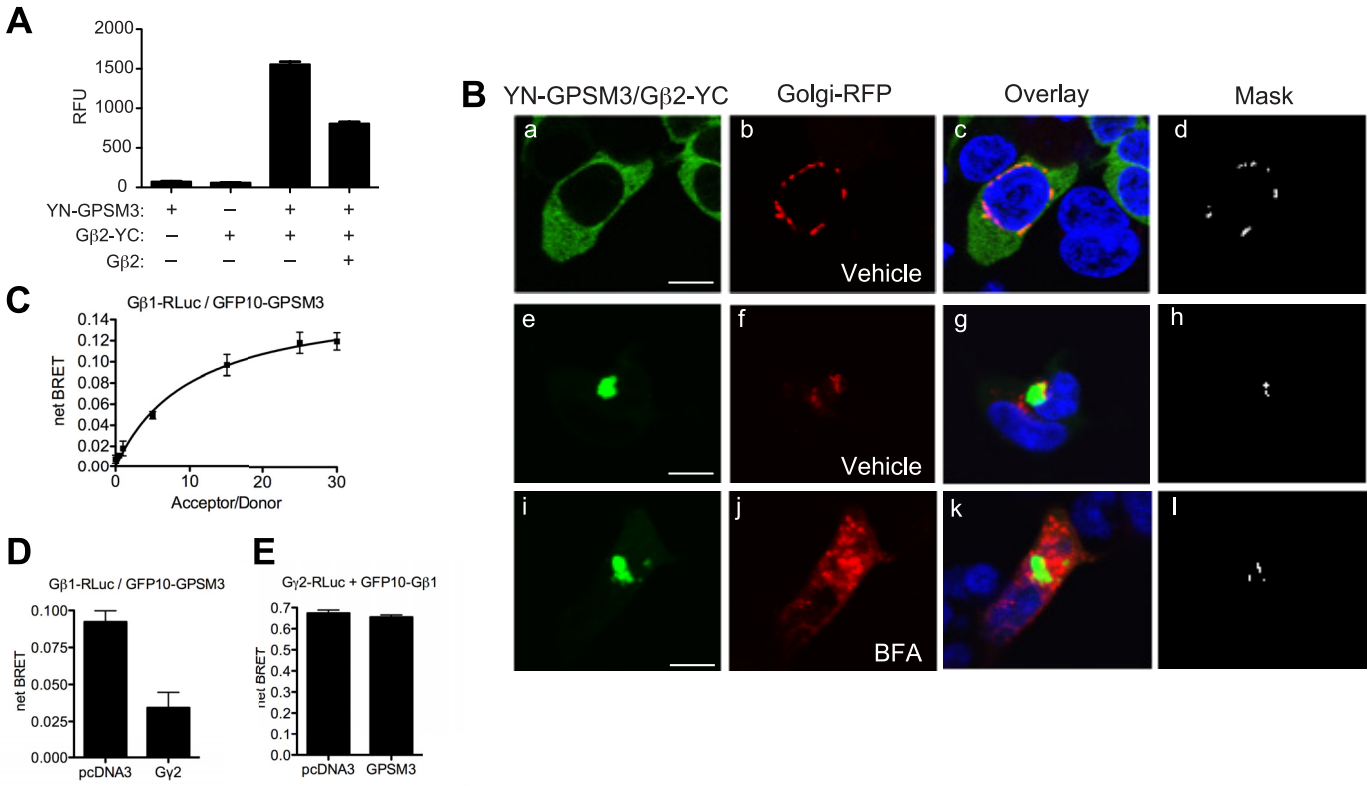

FIGURE 3. **Analysis of GPSM3 and Gβ interaction using BiFC and BRET.** *A* and *B*, HEK293 were transfected with plasmids expressing YN-GPSM3 (amino acids 1–158 of YFP fused to GPSM3) and Gβ2-YC (Gβ2 fused to amino acids 159–238 of YFP) and the fluorescence reconstituted YFP fluorophore was assayed at 24 h post-transfection. *A*, cells were harvested and fluorescence quantified on a plate reader. Total DNA used for transfection was normalized using empty pcDNA3.1 vector DNA. Data are expressed as relative fluorescence units (*RFU*) using the means ± S.E. of at least three different experiments. *B*, confocal microscopy images of HEK293 cells transfected with plasmids expressing the two YFP protein fragment fusions (*panels a, e,* and *i*) and Golgi-RFP (*panels b, f,* and *j*). *Panels a* and *e* show the two different subcellular localization patterns (cytosolic and juxtanuclear) observed for the YN-GPSM3/Gβ2-YC complex. *Panels i, j, k,* and *l* represent cells treated with BFA prior to fixation. BFA was seen to disperse the Golgi apparatus (*panel j*) but only partially disperse the YN-GPSM3/Gβ2-YC complex from its juxtanuclear position. *Panels c, g,* and *k* represent the fluorescence signal from the YN-GPSM3/Gβ2-YC complex overlaid with the Golgi-RFP marker signal, and *panels d, h,* and *l* represent the corresponding co-localization as assessed by extracting co-incident pixels from each fluorophore signal (*Mask*). The *bar* represents 10 μm in all images. *C*, interaction between GSPM3 and Gβ was also confirmed by a BRET saturation experiment. A constant amount of Gβ1-RLuc fusion expression vector was co-transfected into HEK293 cells with increasing amounts of GFP10-GPSM3 fusion expression vector; the resultant net BRET ratio was plotted as a function of the acceptor/donor ratio. The specificity of the interaction is indicated by the saturable nature of the BRET signal. *D* and *E*, co-expression of Gγ2 is presumed to displace GPSM3 from its Gβ subunit interaction, as suggested by a reduction of the BRET signal between Gβ1-RLuc and GFP10-GPSM3 fusion (*D*), although co-expression of untagged GPSM3 was not seen to perturb the BRET signal obtained from the Gγ2-RLuc/GFP10-Gβ1 fusion pair (*E*), suggesting that the GPSM3 interaction with Gβ subunits occurs before formation of the Gβγ dimer.

untagged Gγ2 greatly diminished the BRET signal detected between Gβ1-RLuc and GFP10-GPSM3 (Fig. 3*D*). Conversely, expression of untagged GPSM3 did not affect the BRET signal between Gγ2-RLuc and GFP10-Gβ1 fusions (Fig. 3*E*), similar to the co-immunoprecipitation data of Fig. 2*C* and supporting the idea that GPSM3 interacts with Gβ before formation of the Gβγ dimer such that GPSM3 cannot induce dissociation of the tight Gβγ dimer.

Gβ-GPSM3 Complex Associates with PhLP and CCT7 and Stabilizes the Gβ Moiety—Several studies have shown that Gβ and Gγ subunits traffic through the Golgi apparatus where they associate together in a process involving chaperone proteins such as PhLP, T-complex protein 1 subunit eta (CCT7), and DRiP78 (38–40). Once properly folded, Gβγ dimers then translocate to the plasma membrane. We found that when co-expressed with Myc-Gβ2, FLAG-tagged GPSM3 can co-immunoprecipitate with PhLP (Fig. 4*A*), a protein known to bind directly to isolated (*i.e.* non-Gγ-complexed) Gβ subunits (29, 38). We were also able to co-immunoprecipitate the CCT7 subunit with FLAG-GPSM3 when HA-Gβ2 was co-expressed (Fig. 4*B*). CCT7 is a subunit of the cytosolic chaperonin containing T-complex polypeptide 1 (CCT)/TRiC group II chaperonin that assists in folding of newly synthesized WD40-containing proteins such as Gβ subunits (41). Both PhLP and CCT7 were initially detected as GPSM3-interacting proteins in our yeast two-hybrid screen. These results support the idea that GPSM3 and Gβ associate early during Gβ biosynthesis and prior to Gβγ dimer assembly.

DRiP78 is known to associate with neosynthesized Gγ, serving as a chaperone-like molecule to stabilize Gγ in a conformation suitable for proper assembly with Gβ (40). We thus used an approach similar to that of DRiP78/Gγ interaction studies to quantify the effect of GPSM3 on Gβ stabilization, namely measuring the cellular fluorescence of GFP-tagged Gβ in the absence or presence of cycloheximide (blocking *de novo* protein synthesis). As observed previously (40), co-expression of Gγ2 stabilized GFP10-tagged Gβ1 from degradation (Fig. 4*C*, *bar 1 versus 2*). Co-expression of GFP10-Gβ1 with GPSM3 was also found to stabilize the Gβ subunit, to a higher degree than Gγ2 co-expression (Fig. 4*C*, *bars 1–3*). Co-expression with Gγ2

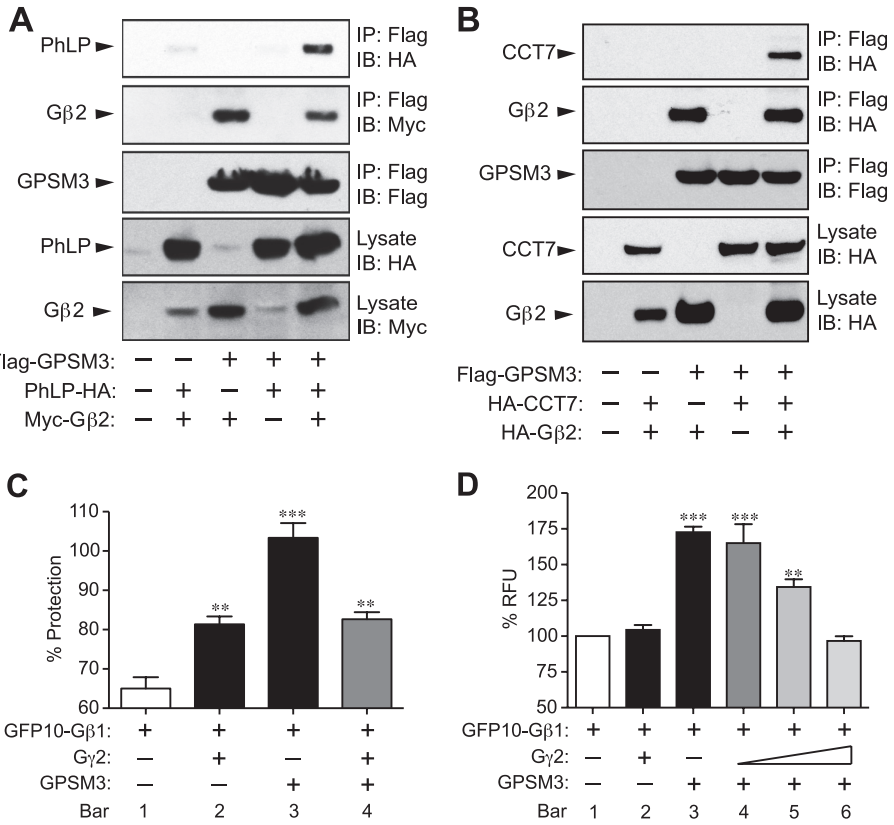

FIGURE 4. **Gβ-GPSM3 complex associates with PhLP and CCT7 and stabilizes the Gβ moiety.** *A* and *B,* to assess the potential interaction between the Gβ-GPSM3 complex and PhLP and CCT7 proteins, HEK293 cells were transiently co-transfected with plasmids expressing the FLAG-tagged GPSM3, HA-tagged PhLP, and Myc-tagged Gβ2 subunit (*A*) or the FLAG-tagged GPSM3, HA-tagged CCT7, and HA-tagged Gβ2 subunit (*B*) as indicated. Immunoprecipitation (*IP*) of GPSM3 was performed using agarose-conjugated anti-FLAG M2 antibody, and co-immunoprecipitating proteins were detected by immunoblotting (*IB*) with anti-HA or -Myc epitope tag antibodies. *C* and *D,* GFP10-Gβ1 was co-expressed with either empty vector (pcDNA3.1), Gγ2, GPSM3, or GPSM3 and Gγ2 together to verify the effect of these proteins on GFP10-Gβ_1 stability. Cells were transfected and 24 h post-transfection were treated with cycloheximide (150 μg/ml) (*C*) or not (*D*) for 3 h prior to harvesting and measurement of total GFP fluorescence. Data are expressed as % of total fluorescence measured before cycloheximide treatment (*C, % protection*) or to GFP10-Gβ1 transfected alone (*D, % RFU* (relative fluorescence units)). The means ± S.E. of at least three different experiments are plotted; *, $p < 0.05$; **, $p < 0.01$, and ***, $p < 0.001$ by one-way ANOVA.

along with GPSM3 was observed to reduce the stabilization effect of GPSM3 to the level observed with Gγ alone (Fig. 4*C, bars 2–4*), supporting the notion that Gγ likely displaces GPSM3 from Gβ (consistent with the results of Figs. 2 and 3 suggesting mutually exclusive Gβ-GPSM3 and Gβγ complexes).

During these stability/protection experiments, we found the basal fluorescence of GFP10-Gβ1 (*i.e.* before blocking protein synthesis with cycloheximide) was affected dramatically by GPSM3 co-expression, whereas Gγ expression had no effect on fluorescence intensity (*e.g.* Fig. 4*D*, *bars 1* and *2 versus 3*). We used this phenomenon to observe that the influence of Gγ expression superseded that of GPSM3, given that graded reductions in GFP10-Gβ1 fluorescence enhancement were seen upon greater quantities of *Gγ2* cDNA co-transfected with GPSM3 and GFP10-Gβ1 (Fig. 4*D*, *bars 4–6*). Taken together, these experiments suggest that GPSM3 interacts with and thereby stabilizes Gβ, and this interaction occurs until Gγ displaces GPSM3 to form the mature Gβγ dimer. The absence of an effect by Gγ2 overexpression on the basal fluorescence intensity of overexpressed GFP10-Gβ1 likely reflects that, once the Gβγ complex is formed, it is subjected to normal turnover as a native and functional complex.

Detection of an Endogenous Gβ/GPSM3 Interaction in Monocytic THP-1 Cell Line—Further establishing the Gβ/GPSM3 interaction, we were able to co-immunoprecipitate endogenous Gβ subunits along with endogenous GPSM3 from THP-1 cell lysate using our anti-GPSM3 monoclonal antibody 35.5.1 (Fig. 5*A, inset*). As detected by confocal microscopy using a commercial pan-Gβ antibody, endogenous Gβ subunits were co-localized with GPSM3 at the plasma membrane in THP-1 cells (Fig. 5*A*). Juxtanuclear intracellular pools of the two proteins were also detected that correspond to a Golgi proximal complex (Fig. 5*A, Mask panel*, *arrows*), as also observed in the BiFC overexpression experiments.

Plasma membrane co-localization of endogenous Gβ and GPSM3 proteins in THP-1 cells is consistent with the recent report from Oner *et al.* (21) in which GPSM3 was shown (by BRET analyses) to be capable of forming a G-protein-dependent complex in proximity to plasma membrane-delimited GPCRs (*i.e.* the α_2-adrenergic receptor). We confirmed a plasma membrane-delimited association between GPSM3 and Gβ subunits using an imaging FRET approach in HEK293 cells. Venus-tagged GPSM3 was co-expressed with cyan fluorescent protein-tagged Gβ2 and analyzed by FRET acceptor photobleaching (42). This approach measures donor "de-quenching"

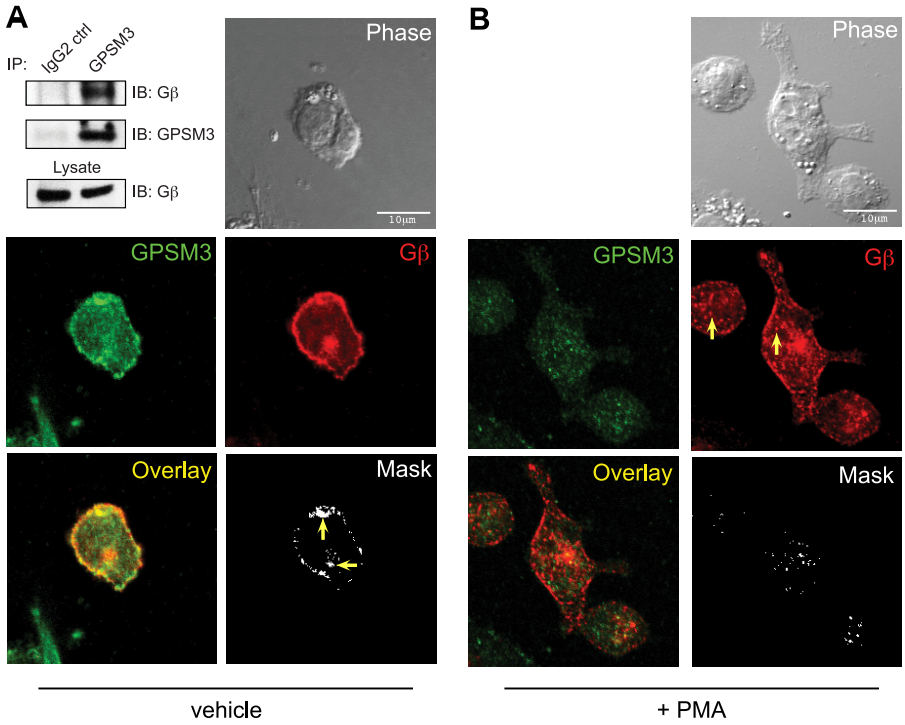

FIGURE 5. **Endogenous GPSM3 is co-localized with endogenous Gβ subunits at plasma membrane and juxtanuclear positions in THP-1 cells.** Endogenous GPSM3 was detected in untreated (*A*) and PMA-differentiated (*B*) THP-1 cells by confocal microscopy using indirect immunofluorescence staining with anti-GPSM3 monoclonal antibody 35.5.1 and FITC-labeled anti-mouse secondary antibody; endogenous Gβ subunits were concomitantly detected with a rabbit polyclonal pan-Gβ antibody and Texas Red-labeled anti-rabbit secondary antibody. Gβ/GPSM3 co-localization was assessed by extracting the co-incident pixels from each fluorophore signal (*Mask*). *Inset*, whole cell lysate from THP-1 cells was immunoprecipitated (*IP*) with the anti-GPSM3 mouse monoclonal antibody 35.5.1 or an IgG2 isotype control (*ctrl*); endogenous Gβ subunits were subsequently detected using a pan-Gβ subunit antibody. *IB*, immunoblot. *Scale bar*, 10 μm.

after destruction of the acceptor by photobleaching. The supplemental Fig. S2 illustrates that increased FRET efficiency was observed both at the plasma membrane and in the cytoplasm.

As the monocytic THP-1 cell line can be easily differentiated to macrophage-like cells via phorbol ester treatment (43–45), we examined the cellular distribution of GPSM3 and Gβ subunits following this process. THP-1 cells were differentiated with PMA for 72 h and immunostained for endogenous GPSM3 and Gβ expression (Fig. 5*B*). Differentiated THP-1 cells showed a clear reduction of GPSM3 immunostaining, with the remaining staining localized in the cytoplasm as punctate structures. We found a similar redistribution of Gβ subunits, although overall expression was not affected (Fig. 5*B*). Gβ relocalization to cytoplasmic puncta co-localizes with the remaining GPSM3 signal, as observed in the *Mask panel* of Fig. 5*B*.

Gβ/GPSM3 Interaction Is Not Dependent on the Gα$_i$·GDP/GoLoco Motif Interaction—A simple explanation for the Gβ/GPSM3 interaction could potentially be found in the known association of GPSM3 GoLoco motifs with inactive-state Gα$_i$·GDP subunits (19, 20), the latter proteins being well established as high affinity binding partners for Gβγ dimers when in this particular nucleotide state (33). However, biochemical, cellular, and structural analyses of the Gα$_i$·GDP/GoLoco motif interaction have strongly suggested mutual exclusion of this interaction *versus* formation of the Gα$_i$·GDP/Gβγ heterotrimer (14, 15). Yet, more recently, evidence of a second high affinity Gβγ-binding site on Gα$_{i1}$·GDP has been reported (46). To exclude the possibility that the observed Gβ/GPSM3 interaction is somehow brokered by the Gα$_i$·GDP/GoLoco motif interaction, we performed additional co-immunoprecipitation experiments. We produced a GPSM3 loss-of-function double point mutant (called "RF") in which both arginines that are part of the critical GoLoco triad motif ((E/D)Q**R**) of the active GoLoco motifs GL1 and GL3 (Arg-81 and Arg-152) were mutated to phenylalanine. This Arg-to-Phe point mutation eliminates binding of Gα$_i$ subunits to GoLoco motifs (13, 14), including both of the active GoLoco motifs within GPSM3 (19). Fig. 6*A* presents co-immunoprecipitation results re-affirming that the double GoLoco mutant GPSM3 exhibits greatly reduced binding to Gα$_{i1}$ subunits. This double GoLoco mutant was then used to evaluate whether or not Gα$_i$ could bridge the interaction between Gβ and GPSM3. Gβ1 was observed to co-immunoprecipitate with the double Arg-to-Phe GPSM3 mutant as well as with wild-type GPSM3 (Fig. 6*B*, compare *lanes 5* and *8*), excluding the possibility that Gα$_i$ serves as a linker between GPSM3 and Gβ subunits. A reduction in the amount of the Gβ-GPSM3 complex was observed when Gα$_{i1}$ was co-expressed, and this reduction was less pronounced with the RF mutant (Fig. 6*B*, compare *lanes 6* and *9*). This reduction may result from some form of steric hindrance or intramolecular regulation of GPSM3 by the binding of Gα$_{i1}$ to one of its GoLoco motifs, possibilities that will need to be tested in the future using recombinant protein interaction studies.

Identification of a Gβ Interaction Site within GPSM3—From multiple truncation experiments (*e.g.* supplemental Fig. S3), we

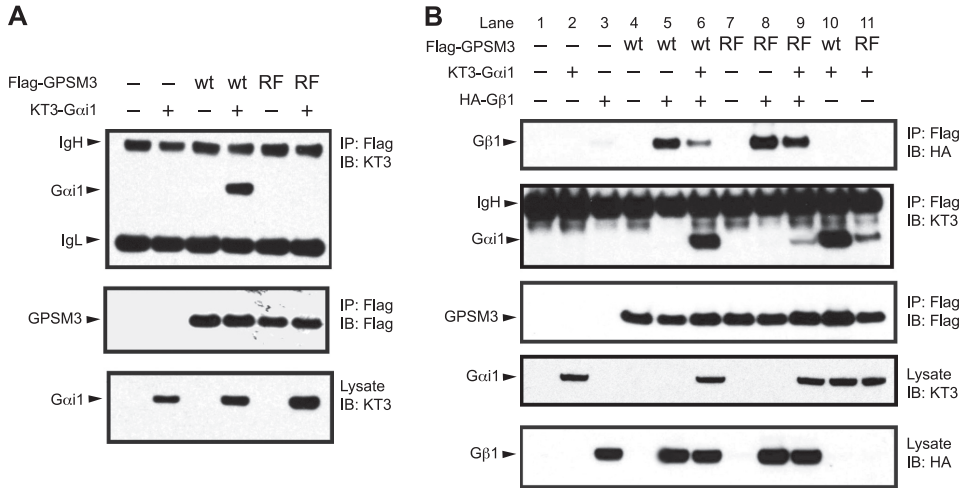

FIGURE 6. **Gβ/GPSM3 interaction is not dependent on the Gα$_i$·GDP/GoLoco motif interaction.** *A,* to validate that Gα$_i$ binding is eliminated by loss-of-function point mutations to the first and third GoLoco motifs of GPSM3 (R81F and R152F, called RF), COS-7 cells were co-transfected with indicated GPSM3 and Gα$_{i1}$ cDNAs and subjected to immunoprecipitation (*IP*) with agarose-conjugated anti-FLAG M2 antibody and immunoblotting (*IB*) with anti-FLAG or anti-KT3 epitope tag antibodies as indicated. *B,* to test for the Gβ/GPSM3 interaction in the absence of functional GoLoco motifs, wild-type or RF mutant GPSM3 cDNA was co-transfected with indicated Gα$_{i1}$ and/or Gβ1 cDNAs into COS-7 cells, and resultant whole cell lysates were subjected to immunoprecipitation and immunoblotting as described for *A*. Immunoglobulin heavy and light chains are denoted *IgH* and *IgL*, respectively.

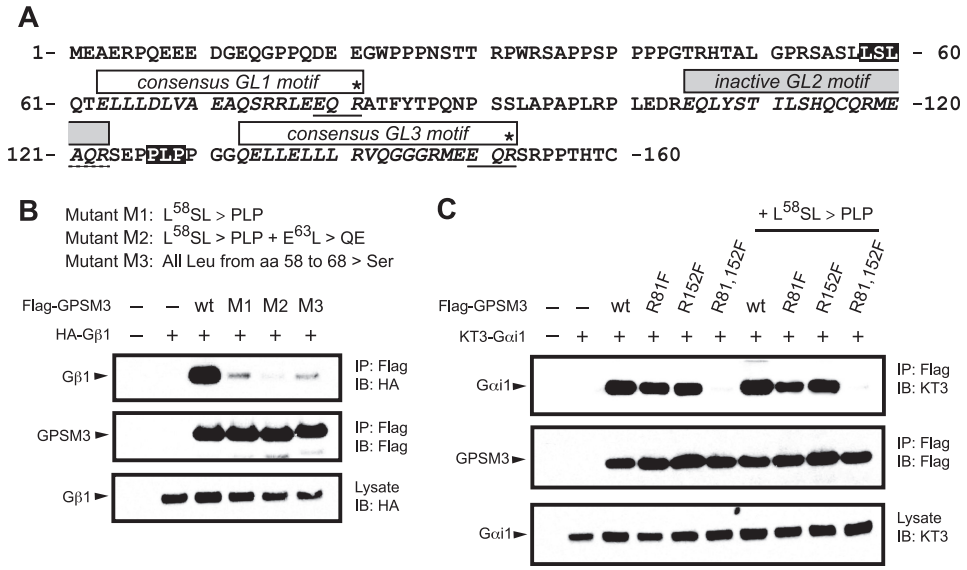

FIGURE 7. **A leucine-rich motif in GPSM3 is critical for Gβ interaction.** *A,* polypeptide sequence of human GPSM3 illustrating locations of the consensus GL1 and GL3 GoLoco motifs (as defined in Ref. 11), the inactive GL2 GoLoco motif lacking the acidic amino acid of the (E/D)QR triad (*dashed underline* in GL2; *solid underline* in GL1 and GL3) (19), and the arginine 81 and 152 residues (*asterisks*) mutated to phenylalanine to eliminate Gα$_i$ binding to the GL1 and GL3 motifs, respectively. The tripeptide sequence ^{58}LSL, N-terminal to the GL1 motif, is displayed in a *black box*, as is the cognate sequence from the same position N-terminal to the GL3 motif. *B* and *C,* COS-7 cells were co-transfected with the indicated cDNA constructs and resultant whole cell lysates subjected to immunoprecipitation (*IP*) with agarose-conjugated anti-FLAG M2 antibody and immunoblotting (*IB*) using indicated antibodies. GPSM3 mutant *M1*, in which the tripeptide sequence ^{58}LSL was replaced with proline-leucine-proline, was observed to nearly eliminate the co-immunoprecipitation of Gβ1 (*B*) but preserve binding to Gα$_{i1}$ (*C*).

were able to discern a minimal Gβ interaction site between amino acids 50 and 70 of GPSM3. This region begins N-terminal to the first GoLoco motif of GPSM3 (GL1; amino acids 63–81) and overlaps with the first eight residues of the GL1 motif (Fig. 7*A*). This region contains multiple leucine residues within a span of a probable α-helix secondary structure (19). Mutation of all leucines between amino acids 58 and 68 either to alanine or to serine, within the context of full-length GPSM3, eliminated interaction with Gβ1 (*e.g.* Fig. 7*B*, "mutant M3"). The extensive number of point mutations, while implicating this leucine-rich hydrophobic region in Gβ binding, also disrupted interaction between Gα$_{i1}$ and the GL1 GoLoco motif (data not shown). As the GL3 region of GPSM3, when tested in isolation, did not show any Gβ interaction (data not shown), we therefore used a sequence alignment of these two active GoLoco motif regions (GL1 *versus* GL3 plus adjoining N-terminal residues) to predict new point mutations that would affect the Gβ interaction without affecting the Gα$_{i1}$/GL1 motif interaction. The GL1 and GL3 motifs are highly conserved, including the first leucine-rich α-helix (Fig. 7*A*), so we focused on the proximal amino acids N-terminal to the GL1 GoLoco motif. This region upstream of the GL1 motif (^{57}LLSLQTEL^{64}) was then mutated to either L**PLP**QTEL or L**PLP**QT**QE** (sequences closer to those found in the GL3 motif region), and

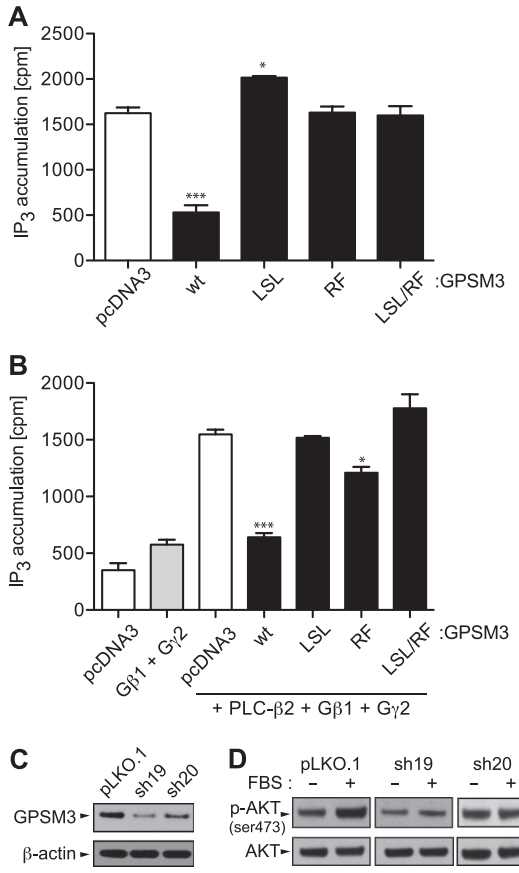

FIGURE 8. **GPSM3 influences Gβγ-mediated signaling to inositol phosphate accumulation and phosphatidylinositol-dependent Akt activation.** *A,* inositol phosphate accumulation upon agonist-induced activation of the lysophosphatidic acid receptor LPA1R was measured in HEK293 cells co-transfected with LPA1R expression vector and the indicated cDNAs. GPSM3 *LSL* and *RF* mutants lack the capacity to interact with Gβ and Gα$_i$ subunits, respectively, as established in Figs. 6 and 7; wild-type GPSM3 is denoted *wt*. *B,* effect of GPSM3 expression on direct activation of PLCβ2 by free Gβ1γ2 dimers was measured by inositol phosphate accumulation assays in COS-7 cells transiently co-transfected with indicated expression plasmids. All values are the means ± S.E. of three separate experiments; *, $p < 0.05$ and ***, $p < 0.001$ by one-way ANOVA. *C* and *D,* activation of Akt, a downstream effect of Gβγ-activated PI3K function, was analyzed in THP-1 cell lines stably infected with a control vector pLKO.1 or with two different shRNA vectors (sh19 and sh20) targeting *GPSM3* for RNA interference knockdown. *C,* whole cell lysate from the three derived cell lines were blotted against endogenous GPSM3, showing reduced expression in the sh19 and sh20 infected THP-1 cell lines. *D,* phosphorylation of Akt on serine 473 following 30 min of treatment with 10% FBS-containing medium was assayed by immunoblotting. Akt activation was only detected in the control pLKO.1 THP-1 cell line and absent in the two cells line with reduced GPSM3 expression.

the resultant full-length GPSM3 constructs were tested for their ability to bind Gβ and Gα$_i$ subunits. The minimal ^{58}LSL^{60}-to-PLP mutation was found to reduce dramatically the interaction with Gβ (Fig. 7*B*, *mutant M1*) while preserving the binding of GPSM3 to Gα$_{i1}$ (Fig. 7*C*).

Role of Gβ/GPSM3 Interaction in Modulating Cellular Signaling—The ^{58}LSL^{60}-to-PLP (called "LSL") mutant of GPSM3 presented the opportunity to investigate the role of the Gβ interaction without affecting Gα$_i$ binding. We returned to examining the effect of GPSM3 on the PLCβ signaling pathway as it is a well established effector of Gβγ dimers (47). Two approaches were used, one via activation of the lysophosphatidic acid receptor LPA1R in cells expressing endogenous PLCβ and the other by ectopic PLCβ2 overexpression. In both cases, overexpression of wild-type GPSM3 was found to inhibit receptor-stimulated inositol phosphate production by >50%, whereas the loss-of-function LSL mutant did not elicit any inhibition (Fig. 8, *A* and *B*). As the primary known function of GPSM3 is to interact with the inactive GDP-bound form of Gα$_i$, we also examined the effect of the double RF mutant, for which Gα$_i$ binding is strongly reduced. The RF mutant was seen to possess a similar loss of inhibitory function as that of the LSL mutant (Fig. 8, *A* and *B*). Reducing the interactions to both Gα$_i$ and Gβ subunits by including both point mutations ("LSL/RF") was found to be equivalently deleterious to the inhibitory function of GPSM3. Thus, both the Gα$_i$·GDP/GoLoco motif and Gβ/GPSM3 interactions are required for the inhibitory effect of GPSM3 on this particular GPCR/effector signal transduction system.

A second and well characterized Gβγ effector is the class IB phosphatidylinositol 3-kinase (PI3K). Once activated, PI3K leads to the generation of plasma membrane-delimited, 3′-phosphorylated phosphatidylinositols and subsequent activation of the downstream effector protein kinase B (PKB or Akt). Phosphorylation of endogenous Akt is an established PI3K-specific read-out system (48). As the p101 regulatory subunit of PI3K is known to bind directly to Gβγ and has a restricted expression to the hematopoietic cell lineage, we also investigated the activation of this pathway in the THP-1 cell line that expresses endogenous levels of GPSM3. We produced two independent THP-1-derived cell lines, each expressing a different shRNA targeting the *GPSM3* transcript, as follows: one targeting the coding sequence (sh19) and the other one targeting the 5′UTR region (sh20). A control THP-1 cell line was generated by infection with lentivirus obtained from empty vector (pLKO.1). Both sh19 and sh20 THP-1 cell lines have a 60% or greater decrease in endogenous GPSM3 expression levels as compared with the control pLKO.1 THP-1 cell line (Fig. 8*C*). Upon serum-starving these cell lines for 2 h and then stimulating with FBS-containing medium for 30 min, the control THP-1 cells exhibited an ~3-fold increase in Akt phosphorylation (Ser-473; Fig. 8*D*); however, both GPSM3-knockdown THP-1 cell lines showed no observable increase in Akt phosphorylation. This evidence of endogenous GPSM3 acting in a pathway involving Gβγ- and phosphatidylinositol-mediated signaling to Akt activation (Fig. 8*D*), coupled with the ability of ectopic GPSM3 expression to suppress Gβγ-mediated inositol phosphate production (Fig. 8, *A* and *B*), suggests a role for GPSM3 in scaffolding and/or coordinating Gβ subunit-dependent cellular signaling.

Conclusions—A role for GPSM3 as a novel regulator of heterotrimer-GPCR complex formation and function is suggested by evidence of GPSM3-mediated stabilization of neosynthesized Gβ, its well described role as a Gα$_i$·GDP-interacting protein, and recent BRET data (coupled with our BiFC, BRET, and FRET results) (21) establishing a proximal complex between GPSM3, G-protein subunits, and the α$_2$-adrenergic receptor. The plasma membrane-spanning nature of GPCRs, and consequent requirement for lipid modification of heterotrimeric G-protein subunits for efficient assembly with GPCRs, adds complexity to the subcellular routing by which G-proteins, receptors, and effectors assemble together after their initial

synthesis (49, 50). The timing and subcellular localization of assembly events may influence the composition of the mature signaling complex and hence determine its specificity. How the Gα subunit is recruited to the nascent Gβγ dimer to initially create the heterotrimer is still not clear (49), nor are the cellular mechanisms by which specificity is achieved among the multiple couplings possible between Gα, Gβ, and Gγ subunits. In this context, GPSM3 may represent a G-protein subunit co-chaperone or scaffold that fosters integration of different elements, including receptor and G-protein α and βγ subunits, to form a functional signaling unit, as well as squelches inappropriate signaling by acting on Gα (through its GoLoco motif guanine nucleotide dissociation inhibitor activity) until it forms the mature heterotrimer with newly assembled Gβγ.

The presence of GPSM3 at the plasma membrane, highlighted in this study as well as a previous report showing regulation of the GPSM3-Gα$_i$ complex formation by agonist-stimulated GPCRs (21), suggests that GPSM3 is not acting solely on Gβ during synthesis but also on G-protein subunits during GPCR activation. It is presently unclear, however, how these Gα$_i$ and Gβ interactions with GPSM3 functionally articulate with regulation of heterotrimeric G-protein dynamics and GPCR signaling. Intracellular GPSM3 could also participate in noncanonical signaling by G-proteins other than at the plasma membrane (39).

Our present discovery of a Gβ/GPSM3 interaction should help further elucidate the physiological role of GPSM3 in G-protein signal transduction and may foreshadow GPSM3 as an interesting target for the selective modulation of G-protein signaling in the immune system.[3]

Acknowledgments—The GFP10-Gβ1 construct and BiFC backbone vectors were kind gifts of Dr. Denis J. Dupré (Dept. of Pharmacology, Dalhousie University, Halifax, Nova Scotia, Canada). We thank Dr. Noah Sciaky for assistance with the FRET studies and the North Carolina Biotechnology Center for provision of the Olympus Fluoview 1000 microscope.

REFERENCES

1. Bockaert, J., and Pin, J. P. (1999) Molecular tinkering of G protein-coupled receptors. An evolutionary success. *EMBO J.* **18,** 1723–1729
2. Gurevich, V. V., and Gurevich, E. V. (2008) Rich tapestry of G protein-coupled receptor signaling and regulatory mechanisms. *Mol. Pharmacol.* **74,** 312–316
3. Luttrell, L. M. (2008) Reviews in molecular biology and biotechnology. Transmembrane signaling by G protein-coupled receptors. *Mol. Biotechnol.* **39,** 239–264
4. McCoy, K. L., and Hepler, J. R. (2009) Regulators of G protein signaling proteins as central components of G protein-coupled receptor signaling complexes. *Prog. Mol. Biol. Transl. Sci.* **86,** 49–74
5. Sato, M., Blumer, J. B., Simon, V., and Lanier, S. M. (2006) Accessory proteins for G proteins. Partners in signaling. *Annu. Rev. Pharmacol. Toxicol.* **46,** 151–187
6. Siderovski, D. P., and Willard, F. S. (2005) The GAPs, GEFs, and GDIs of heterotrimeric G-protein α subunits. *Int. J. Biol. Sci.* **1,** 51–66
7. Chung, K. Y., Rasmussen, S. G., Liu, T., Li, S., DeVree, B. T., Chae, P. S., Calinski, D., Kobilka, B. K., Woods, V. L., Jr., and Sunahara, R. K. (2011) Conformational changes in the G protein G$_s$ induced by the β_2-adrenergic receptor. *Nature* **477,** 611–615
8. Johnston, C. A., and Siderovski, D. P. (2007) Receptor-mediated activation of heterotrimeric G-proteins. Current structural insights. *Mol. Pharmacol.* **72,** 219–230
9. Offermanns, S. (2003) G-proteins as transducers in transmembrane signaling. *Prog. Biophys. Mol. Biol.* **83,** 101–130
10. Neubig, R. R., and Siderovski, D. P. (2002) Regulators of G-protein signaling as new central nervous system drug targets. *Nat. Rev. Drug Discov.* **1,** 187–197
11. Willard, F. S., Kimple, R. J., and Siderovski, D. P. (2004) Return of the GDI. The GoLoco motif in cell division. *Annu. Rev. Biochem.* **73,** 925–951
12. Kimple, R. J., De Vries, L., Tronchère, H., Behe, C. I., Morris, R. A., Gist Farquhar, M., and Siderovski, D. P. (2001) RGS12 and RGS14 GoLoco motifs are Gα$_i$ interaction sites with guanine nucleotide dissociation inhibitor activity. *J. Biol. Chem.* **276,** 29275–29281
13. Peterson, Y. K., Bernard, M. L., Ma, H., Hazard, S., 3rd, Graber, S. G., and Lanier, S. M. (2000) Stabilization of the GDP-bound conformation of G$_i$α by a peptide derived from the G-protein regulatory motif of AGS3. *J. Biol. Chem.* **275,** 33193–33196
14. Kimple, R. J., Kimple, M. E., Betts, L., Sondek, J., and Siderovski, D. P. (2002) Structural determinants for GoLoco-induced inhibition of nucleotide release by Gα subunits. *Nature* **416,** 878–881
15. Webb, C. K., McCudden, C. R., Willard, F. S., Kimple, R. J., Siderovski, D. P., and Oxford, G. S. (2005) D$_2$ dopamine receptor activation of potassium channels is selectively decoupled by Gα-specific GoLoco motif peptides. *J. Neurochem.* **92,** 1408–1418
16. Siderovski, D. P., Diversé-Pierluissi, M., and De Vries, L. (1999) The GoLoco motif. A Gα$_{i/o}$-binding motif and potential guanine nucleotide exchange factor. *Trends Biochem. Sci.* **24,** 340–341
17. Ponting, C. P. (1999) Raf-like Ras/Rap-binding domains in RGS12- and still life-like signaling proteins. *J. Mol. Med.* **77,** 695–698
18. Takesono, A., Cismowski, M. J., Ribas, C., Bernard, M., Chung, P., Hazard, S., 3rd, Duzic, E., and Lanier, S. M. (1999) Receptor-independent activators of heterotrimeric G-protein signaling pathways. *J. Biol. Chem.* **274,** 33202–33205
19. Kimple, R. J., Willard, F. S., Hains, M. D., Jones, M. B., Nweke, G. K., and Siderovski, D. P. (2004) Guanine nucleotide dissociation inhibitor activity of the triple GoLoco motif protein G18. Alanine-to-aspartate mutation restores function to an inactive second GoLoco motif. *Biochem. J.* **378,** 801–808
20. Cao, X., Cismowski, M. J., Sato, M., Blumer, J. B., and Lanier, S. M. (2004) Identification and characterization of AGS4. A protein containing three G-protein regulatory motifs that regulate the activation state of G$_i$α. *J. Biol. Chem.* **279,** 27567–27574
21. Oner, S. S., Maher, E. M., Breton, B., Bouvier, M., and Blumer, J. B. (2010) Receptor-regulated interaction of activator of G-protein signaling-4 and Gα$_i$. *J. Biol. Chem.* **285,** 20588–20594
22. Johnston, C. A., Taylor, J. P., Gao, Y., Kimple, A. J., Grigston, J. C., Chen, J. G., Siderovski, D. P., Jones, A. M., and Willard, F. S. (2007) GTPase acceleration as the rate-limiting step in *Arabidopsis* G protein-coupled sugar signaling. *Proc. Natl. Acad. Sci. U.S.A.* **104,** 17317–17322
23. Lambert, N. A., Johnston, C. A., Cappell, S. D., Kuravi, S., Kimple, A. J., Willard, F. S., and Siderovski, D. P. (2010) Regulators of G-protein signaling accelerate GPCR signaling kinetics and govern sensitivity solely by accelerating GTPase activity. *Proc. Natl. Acad. Sci. U.S.A.* **107,** 7066–7071
24. Zhao, P., Nguyen, C. H., and Chidiac, P. (2010) The proline-rich N-terminal domain of G18 exhibits a novel G protein regulatory function. *J. Biol. Chem.* **285,** 9008–9017
25. Jordan, J. D., Carey, K. D., Stork, P. J., and Iyengar, R. (1999) Modulation of rap activity by direct interaction of Gα$_o$ with Rap1 GTPase-activating protein. *J. Biol. Chem.* **274,** 21507–21510
26. Luo, Y., and Denker, B. M. (1999) Interaction of heterotrimeric G protein Gα$_o$ with Purkinje cell protein-2. Evidence for a novel nucleotide exchange factor. *J. Biol. Chem.* **274,** 10685–10688
27. Mochizuki, N., Cho, G., Wen, B., and Insel, P. A. (1996) Identification and cDNA cloning of a novel human mosaic protein, LGN, based on interaction with Gα$_{i2}$. *Gene* **181,** 39–43
28. Sondek, J., and Siderovski, D. P. (2001) Gγ-like (GGL) domains. New frontiers in G-protein signaling and β-propeller scaffolding. *Biochem. Pharmacol.* **61,** 1329–1337
29. Lukov, G. L., Hu, T., McLaughlin, J. N., Hamm, H. E., and Willardson,

B. M. (2005) Phosducin-like protein acts as a molecular chaperone for G protein βγ dimer assembly. *EMBO J.* **24,** 1965–1975
30. Willardson, B. M., and Howlett, A. C. (2007) Function of phosducin-like proteins in G protein signaling and chaperone-assisted protein folding. *Cell. Signal.* **19,** 2417–2427
31. Kerppola, T. K. (2008) Bimolecular fluorescence complementation (BiFC) analysis as a probe of protein interactions in living cells. *Annu. Rev. Biophys.* **37,** 465–487
32. Westwick, J. K., and Michnick, S. W. (2006) Protein-fragment complementation assays (PCA) in small GTPase research and drug discovery. *Methods Enzymol.* **407,** 388–401
33. Gilman, A. G. (1987) G proteins. Transducers of receptor-generated signals. *Annu. Rev. Biochem.* **56,** 615–649
34. Clapham, D. E., and Neer, E. J. (1997) G protein βγ subunits. *Annu. Rev. Pharmacol. Toxicol.* **37,** 167–203
35. Lippincott-Schwartz, J., Yuan, L. C., Bonifacino, J. S., and Klausner, R. D. (1989) Rapid redistribution of Golgi proteins into the ER in cells treated with brefeldin A. Evidence for membrane cycling from Golgi to ER. *Cell* **56,** 801–813
36. Johnston, J. A., Ward, C. L., and Kopito, R. R. (1998) Aggresomes. A cellular response to misfolded proteins. *J. Cell Biol.* **143,** 1883–1898
37. Saliba, R. S., Munro, P. M., Luthert, P. J., and Cheetham, M. E. (2002) The cellular fate of mutant rhodopsin: quality control, degradation, and aggresome formation. *J. Cell Sci.* **115,** 2907–2918
38. Humrich, J., Bermel, C., Bünemann, M., Härmark, L., Frost, R., Quitterer, U., and Lohse, M. J. (2005) Phosducin-like protein regulates G-protein βγ folding by interaction with tailless complex polypeptide-1α. Dephosphorylation or splicing of PhLP turns the switch toward regulation of Gβγ folding. *J. Biol. Chem.* **280,** 20042–20050
39. Hewavitharana, T., and Wedegaertner, P. B. (2012) Noncanonical signaling and localizations of heterotrimeric G proteins. *Cell. Signal.* **24,** 25–34
40. Dupré, D. J., Robitaille, M., Richer, M., Ethier, N., Mamarbachi, A. M., and Hébert, T. E. (2007) Dopamine receptor-interacting protein 78 acts as a molecular chaperone for Gγ subunits before assembly with Gβ. *J. Biol. Chem.* **282,** 13703–13715
41. Kubota, S., Kubota, H., and Nagata, K. (2006) Cytosolic chaperonin protects folding intermediates of Gβ from aggregation by recognizing hydrophobic β-strands. *Proc. Natl. Acad. Sci. U.S.A.* **103,** 8360–8365
42. Kenworthy, A. K. (2001) Imaging protein-protein interactions using fluorescence resonance energy transfer microscopy. *Methods* **24,** 289–296
43. Tsuchiya, S., Kobayashi, Y., Goto, Y., Okumura, H., Nakae, S., Konno, T., and Tada, K. (1982) Induction of maturation in cultured human monocytic leukemia cells by a phorbol diester. *Cancer Res.* **42,** 1530–1536
44. Schwende, H., Fitzke, E., Ambs, P., and Dieter, P. (1996) Differences in the state of differentiation of THP-1 cells induced by phorbol ester and 1,25-dihydroxyvitamin D_3. *J. Leukocyte Biol.* **59,** 555–561
45. Daigneault, M., Preston, J. A., Marriott, H. M., Whyte, M. K., and Dockrell, D. H. (2010) The identification of markers of macrophage differentiation in PMA-stimulated THP-1 cells and monocyte-derived macrophages. *PLoS ONE* **5,** e8668
46. Wang, J., Sengupta, P., Guo, Y., Golebiewska, U., and Scarlata, S. (2009) Evidence for a second, high affinity Gβγ-binding site on $G\alpha_1$ (GDP) subunits. *J. Biol. Chem.* **284,** 16906–16913
47. Rhee, S. G., and Bae, Y. S. (1997) Regulation of phosphoinositide-specific phospholipase C isozymes. *J. Biol. Chem.* **272,** 15045–15048
48. Brock, C., Schaefer, M., Reusch, H. P., Czupalla, C., Michalke, M., Spicher, K., Schultz, G., and Nürnberg, B. (2003) Roles of G βγ in membrane recruitment and activation of p110γ/p101 phosphoinositide 3-kinase γ. *J. Cell Biol.* **160,** 89–99
49. Dupré, D. J., Robitaille, M., Rebois, R. V., and Hébert, T. E. (2009) The role of Gβγ subunits in the organization, assembly, and function of GPCR signaling complexes. *Annu. Rev. Pharmacol. Toxicol.* **49,** 31–56
50. Marrari, Y., Crouthamel, M., Irannejad, R., and Wedegaertner, P. B. (2007) Assembly and trafficking of heterotrimeric G proteins. *Biochemistry* **46,** 7665–7677